ISTITUTO NAZIONALE DI FISICA NUCLEARE

INFN/BE - 69/8
22 Dicembre 1969

U. Abbondanno, R. Giacomich, L. Granata, M. Lagonegro and G. Pauli:

GAMMA RAYS FOLLOWING THE INELASTIC SCATTERING OF 14.2 MeV NEUTRONS FROM ^{24}Mg, ^{28}Si and ^{56}Fe

GAMMA RAYS FOLLOWING THE INELASTIC SCATTERING OF 14.2 MeV NEUTRONS FROM ^{24}Mg, ^{28}Si and ^{56}Fe

U. Abbondanno, R. Giacomich, L. Granata,
M. Lagonegro and G. Pauli

Istituto di Fisica, Università di Trieste, Italia
Istituto Nazionale di Fisica Nucleare, Sezione di Trieste, Italia

ABSTRACT

Gamma rays resulting from the inelastic scattering of 14.2 MeV neutrons from ^{24}Mg, ^{28}Si and ^{56}Fe have been investigated. The differential cross-sections for the production of the gamma rays of 1.37 MeV from ^{24}Mg, 1.78 MeV from ^{28}Si, 0.85 MeV and 1.24 MeV from ^{56}Fe have been measured and the total cross-sections have been deduced. The incident neutrons were produced by means of the T(d,n) ^{4}He reaction and the associated-particle time-of-flight technique has been used to discriminate between the neutrons and the gamma rays resulting from the inelastic scattering process.

1. - INTRODUCTION

The present work has been undertaken with the aim of providing more complete data on the cross-sections for the production of γ-rays from the inelastic scattering of fast neutrons from various nuclei.

In this experiment the differential cross-sections $\sigma(E_\gamma,\vartheta)$ for the production of the γ-rays of 1.37 MeV from ^{24}Mg, 1.78 MeV from ^{28}Si, 0.85 MeV and 1.24 MeV from ^{56}Fe have been measured for an incident neutron energy of 14.2 MeV, and the absolute yields of these γ rays have been deduced. The nuclei used are all even-A. The γ-rays observed, with the exception of the 1.24 MeV γ-ray from ^{56}Fe, correspond to transitions from 2^+ first excited levels to 0^+ ground levels; the 1.24 MeV γ-ray corresponds to the transition of ^{56}Fe from the second 4^+ to the first 2^+ excited level.

The total cross-sections for the production of these γ-rays for an incident neutron energy of about 14 MeV have been measured by Martin and Stewart ([1]) (E_n = 14.1 MeV), using an associated-particle time-of-flight technique, and by Benetsky and Frank ([2]) (E_n = 14 MeV), by comparison with the cross-sections for the (n,p) reactions. The total cross-section for the production of the 1.37 MeV γ-ray from ^{24}Mg has been measured also by Deuchars and Dandy ([3]) (E_n = 14 MeV), using the time-of-flight technique with pulsed beam and the ring geometry.

The only angular distributions for these γ-rays which have been reported, seem to be those for the 1.37 MeV γ-ray from ^{24}Mg (ref.([4])) and for the 0.85 MeV γ-ray from ^{56}Fe (ref.([5])). Therefore it was felt that information concerning the angular distributions of the γ-rays produced in the two other elements could be of some interest.

2. - EXPERIMENTAL PROCEDURE AND DATA ANALYSIS

The measurements have been performed using the neutrons of the T(d,n)^{4}He reaction, produced by bombarding a titanium-tritium target by 200 keV deuterons. A beam of neutrons of 14.2 MeV energy was defined by means of the associated-particle technique ([6]), by detecting the α particles which

were emitted within a cone of 5° 35'. The neutron energy was defined within ±0.16 MeV.

All the samples used for the measurements were of the natural isotopic mixture. The magnesium and silicon samples were right cylinders 6.1 cm in diameter and 12 cm long. The iron sample was an upright prism 15.6 cm long and with an hexagonal base with the side equal to 1.35 cm. All the samples were placed at a distance of 40 cm from the tritium target.

The γ-rays were detected by means of a 3" × 3" NaI (Tℓ) crystal coupled with a 56 AVP photomultiplier and placed at a distance of 90 cm from the scattering sample. The γ detector was shielded from the neutron source by a conical lead shadow having a length of 50 cm and a circular base 25 cm in diameter.

A time-of-flight technique has been used to distinguish between γ-rays and scattered neutrons produced in the sample by the (n,n'γ) reaction. The discrimination between the γ-rays and the neutrons has been achieved by gating a 200-channel pulse height analyzer, recording the γ-ray events, by means of the pulses contributing to the γ peak in the time-of-flight spectrum and selected with a single-channel analyzer. The coincidence resolution was of 7 nsec.

In order to analyse the background contributions, measurements have been carried out with the single-channel analyzer selecting a part of the time spectrum where neither scattered neutrons nor γ-rays from the reaction could have been expected.

The background affecting the gamma peak was analysed by using a lithium sample. In such region the background was quite similar to that observed outside the γ peak as described above.

The photopeak efficiency of the NaI detector has been determined by means of calibrated γ-sources of ^{22}Na, ^{137}Cs, ^{88}Y, ^{207}Bi, so as to cover the energy range from about 0.5 MeV to about 1.8 MeV.

A typical time-of-flight spectrum, taken at an angle of 45° with respect to the direction of the incident neutron beam, is shown in Fig. 1 for the case of the silicon sample.

The errors quoted on the experimental data include (i) the statistical error (2 to 3 percent), (ii) the error in the determination of the

photopeak efficiency of the detector (3 percent), (iii) the error involved in the evaluation of the photopeak area (4 to 5 percent). The magnitude of the overall error has been estimated to be ±10 percent.

No correction has been made to take the absorption and the multiple scattering of neutrons in the samples into account, since the sizes of the samples were chosen so that this correction was smaller than the error involved in the determination of the photopeak area. This point has been checked by making measurements with a number of samples of different sizes and shapes. The γ-ray attenuation in the samples has been taken into account and a correction for this effect gave an appreciable result only in the case of the iron sample.

3. - EXPERIMENTAL RESULTS

The γ-ray production has been measured at nine angles between 30° and 150° in the laboratory frame of reference. A typical γ-spectrum is shown in Fig. 2.

The total cross-sections for the production of the γ-rays have been deduced by integrating the angular distributions after having extrapolated the experimental data to 0° and to 180°. The error assigned to the values obtained in this way include both the experimental error previously mentioned and the error due to the extrapolation to the extreme angles. This last error has been taken equal to the difference between the integrated cross-section deduced by extrapolating the experimental data down to zero at 0° and 180°, and the one obtained by assuming that the angular distribution goes parallel to the horizontal axis beyond the extreme measured angles.

3.1 The nucleus ^{24}Mg.

The differential cross-section values for the 1.37 MeV γ-ray from ^{24}Mg are plotted in Fig. 3. For the sake of comparison, the data of Ste-

wart and Martin ([4]) are displayed on the same figure (*). The value of the integrated cross-section $\sigma(E_\gamma = 1.37$ MeV), derived in the manner described above, is reported in Table 1. In the same table are listed the previously published ([1,2,3]) cross-sections for the neutron energy under present consideration.

For completness sake, in Table 1 have been listed also the non-elastic cross-sections σ_{nX}, and the available cross-sections for the various non-elastic processes which can be produced by neutrons of 14 MeV energy, as it is indicated by the Q-values reported in Table 2.

From a measurement of the angular distribution of the inelastically scattered neutrons, Clarke and Cross ([7]) deduced for the first level excitation cross-section for ^{24}Mg a value of 168±25 mb. By subtracting this cross-section from the total cross-section for the production of the γ-ray due to de-excitation of the 1.37 MeV level in ^{24}Mg, there remain about 440 mb which should be ascribed to inelastic processes exciting higher levels of ^{24}Mg and cascading through the 1.37 MeV state.

3.2 The nucleus ^{28}Si.

The differential cross-section values for the 1.78 MeV γ-ray from ^{28}Si are shown in Fig. 4. The value of the total cross-section $\sigma(E_\gamma = 1.78$ MeV) is reported in Table 1.

By taking the first level excitation cross-section to be 109±16 mb from the work of Clark and Cross ([7]) or 93±10 mb from the work of Höhn et al.([8]), it turns out that, as for ^{24}Mg, about two thirds of the total cross-section for the production of the γ-ray of de-excitation of the first level is due to cascade decay processes from higher levels.

(*) Such data have been derived from Fig. 4 of ref. ([4]).

3.3 The nucleus ^{56}Fe.

The differential cross-sections for the 0.85 MeV γ-ray and for the 1.24 MeV γ-ray from ^{56}Fe are shown in Fig. 5. The values of the total cross-sections $\sigma(E_\gamma = 0.85\ MeV)$ and $\sigma(E_\gamma = 1.24\ MeV)$ are reported in Table 1.

4. - CONCLUSIONS

Attempts to fit the observed angular distributions of the γ-rays following an $(n,n'\gamma)$ reaction have been made for the 6.1 MeV γ-ray from the 3^- state of ^{16}O using a plane-wave Born calculation ([22]), and for the 1.37 MeV γ-ray from the 2^+ state of ^{24}Mg using the statistical model([4]).

The angular distribution of γ-rays following inelastic neutron scattering can be calculated in terms of the direct reaction mechanism ([23]) provided the angular distribution of the outgoing nucleons is known; the predicted angular distribution can be compared with the observed one provided the latter does not contain contributions from cascade events. While in the case of the 6.1 MeV γ-rays from ^{16}O both these conditions are reasonably verified and a theoretical fit can be carried out as shown in ref.([22]), in the case of the γ-rays from ^{28}Si and ^{24}Mg, studied in the present work, it has to be noticed that their production cross-sections are about three times as large as the neutron inelastic cross-sections for the 2^+ level ([7,8]) and therefore must contain a strong contribution from cascade events. In the case of the γ-rays from ^{56}Fe, on the other hand, the calculations should be based upon a relatively poor knowledge of the inelastic neutron scattering differential cross-sections ([24]).

The prediction of the angular distribution of γ-rays following inelastic neutron scattering can be performed using the continuum theory of nuclear reactions ([25]) provided one knows all the reaction channels which are open and calculates the corresponding penetrabilities. Now, when the energy of the incident neutrons is relatively high, as in the present work, the open channels are not only those for the inelastic neutron scattering, but also for other processes like (n,p), (n,α) and (n,2n). In the

case of the γ-rays studied in the present work, an attempt of calculation (which is not reported here) has been performed, which gave an almost isotropic angular distribution in contrast with the experimental evidence and values for the γ-rays production cross-sections too low in comparison with the measured ones.

As pointed out by other authors ([4]), the inelastic neutron scattering process in the energy range of 14 MeV is presumably due to both the reaction mechanisms, i.e., the compound nucleus scattering and the surface scattering. A systematic investigation of the process studying not only the γ-ray excitation but also the γ-γ and γ-n' coincidences and angular correlations seems highly desirable in order to check the validity of current calculations.

The authors are indebted to Professor G. Poiani for his interest in this work.

References

(1) P.W. Martin and D.T. Stewart, Can. Journ. of Phys. 46 (1968) 1657.

(2) B.A. Benetsky and I.M. Frank, C.R. du Congrès International de Physique Nucléaire (Centre Nat.Res.Sci., Paris, 1964) p. 817.

(3) W.M. Deuchars and D. Dandy, Proc. Phys. Soc. 75 (1960) 855.

(4) D.T. Stewart and P.W. Martin, Nucl. Phys. 60 (1964) 349.

(5) P.W. Martin and D.T. Stewart, Journ. Nucl. Energy 19 (1965) 447.

(6) L. Granata and M. Lagonegro, Nucl. Instr. and Meth. 70 (1969) 93.

(7) R.L. Clarke and W.G. Cross, Nucl. Phys. 53 (1964) 177.

(8) J. Höhn, H. Pose D. Seelinger and R. Reif, Nucl. Phys. A134 (1969) 289.

(9) M.H. McGregor, W.P. Ball and R. Booth, Phys. Rev. 108 (1957) 726.

(10) P. Cuzzocrea, S. Notarrigo and E. Perillo, Report INFN/BE-67/10.

(11) F.C. Engesser and W.E. Thompson, Journ. Nucl. Energy 21 (1967) 487.

(12) A. Chattarjee, Phys. Rev. 134 B (1964) 374; Nucl. Phys. 47 (1963) 617.

(13) N.N. Flerov and V.M. Talyzin, Atomic Energy (U.S.S.R.), 4 (1956) 617.

(14) H. Morgenstern, D. Hilscher and J. Scheer, Nucl. Phys. 83 (1966) 369.

(15) D.L. Allan, Nucl. Phys. 24 (1961) 274.

(16) L. Colli, I. Iori, S. Micheletti and M. Pignanelli, Nuovo Cimento 20 (1961) 95.

(17) M. Bormann, Nucl. Phys. 65 (1965) 257.

(18) P. Cuzzocrea, E. Perillo and S. Notarrigo, Nuovo Cimento B54 (1968) 53.

(19) L. Colli, E. Gadioli, S. Micheletti and D. Luciani, Nucl. Phys. 46 (1963) 73.

(20) C. Maples, G.W. Goth and I. Cerny, Nuclear Reaction Q-values (University of California, Berkeley, 1966), UCRL 16964.

(21) F. Everling, L.A. Koenig, J.H.E. Mattauch and A.H. Wapstra, 1960 Nuclear Data Tables (National Academy of Sciences, Washington, 1961) Part I.

(22) W.J. McDonald, J.M. Robson and R. Malcom, Nucl. Phys. 75 (1966) 353.

(23) G.R. Satchler, Proc. Phys. Soc. A68 (1955) 1037.

(24) G.C. Bonassola, T. Bressani, P. Brovetto, E. Chiavassa and R. Demicheli, Nucl. Phys. 51 (1964) 353.

(25) G.R. Satchler, Phys. Rev. 104 (1956) 1198.

Table 1

Cross-sections for non-elastic reactions.

Element	$\sigma_{n,X}$ (mb)	$\sigma_{n,n'}(E_\gamma)$ (mb)	E_γ (MeV)	$\sigma_{n,p}$ (mb)	$\sigma_{n,\alpha}$ (mb)	$\sigma_{n,np}$ (mb)	$\sigma_{n,d}$ (mb)	$\sigma_{n,2n}$ (mb)
^{24}Mg	990 ± 20 [a]	605 ± 60 [b] 619 ± 60 [c] 590 ± 90 [d] 550 ± 100 [e]	1.37	185 ± 21 [f]	146 [g] 55 [h]			
^{28}Si	1020 ± 60 [i]	360 ± 40 [b] 471 ± 70 [c] 370 ± 60 [d]	1.78	217 ± 26 [f]	190 ± 40 [l]	27 ± 22 [m]		
^{56}Fe	1360 ± 30 [a]	733 ± 70 [b] 1268 ± 150 [c] 660 ± 80 [d]	0.85	108 ± 11 [f] 123 ± 9 [p]	50 [h]	35 ± 7 [m]	14 [n] 6.4 [q]	440 ± 88 [o]
		420 ± 40 [b] 695 ± 80 [c] 270 ± 40 [d]	1.24					

[a] Ref. (9). [b] Present work. [c] Ref. (1). [d] Ref. (2). [e] Ref. (3). [f] Ref. (10). [g] Obtained by multiplying by 4π the differential cross-section measured at 90° ±20° and given in Ref. (11). [h] Ref. (12). [i] Ref. (13). [l] Obtained by integrating over angle the angular distribution given in Ref. (14). [m] Ref. (15). [n] Obtained by multiplying by 4π the differential cross-section measured at 14° and given in Ref. (16). [o] Ref. (17). [p] Ref. (18). [q] Obtained by multiplying by 4π the differential cross-section measured at 15° and given in Ref. (19).

Table 2

Q-values for the non-elastic reactions which can be induced by neutrons of 14.2 MeV energy in ^{24}Mg, ^{28}Si and ^{56}Fe.

Element	Reaction	Q-value (*) (MeV)
^{24}Mg	(n,p) ^{24}Na	- 4.733
	(n,d) ^{23}Na	- 9.467
	(n,^{3}He) ^{22}Ne	- 12.764
	(n, α) ^{21}Ne	- 2.554
	(n,np) ^{23}Na	- 11.692
^{28}Si	(n,p) ^{28}Al	- 3.856
	(n,d) ^{27}Al	- 9.355
	(n,^{3}He) ^{26}Mg	- 12.135
	(n, α) ^{25}Mg	- 2.655
	(n,np) ^{27}Al	- 11.580
	(n,2p) ^{27}Mg	- 13.415
^{56}Fe	(n,p) ^{56}Mn	- 2.926
	(n,d) ^{55}Mn	- 7.972
	(n,^{3}He) ^{54}Cr	- 10.537
	(n, α) ^{53}Cr	+ 0.319
	(n,2n) ^{55}Fe	- 11.211
	(n,np) ^{55}Mn	- 10.196
	(n,2p) ^{55}Cr	- 12.230
	(n,t) ^{54}Mn	- 11.934

(*) From ref. ([20]) for the nuclear reactions with one outgoing particle.
From ref. ([21]) for the nuclear reactions with two outgoing particles.

Figure Captions

Fig. 1 - Time-of-flight spectrum of scattered neutrons and de-excitation γ rays from the silicon sample.

Fig. 2 - γ ray spectrum for the ^{56}Fe sample.

Fig. 3 - The differential cross-sections for the 1.37 MeV γ ray from ^{24}Mg: • present work, □ data of Stewart and Martin (4).

Fig. 4 - The differential cross-sections for the 1.78 MeV γ ray from ^{28}Si.

Fig. 5 - The differential cross-sections for the 0.85 MeV (•) and 1.24 MeV (Δ) γ rays from ^{56}Fe.

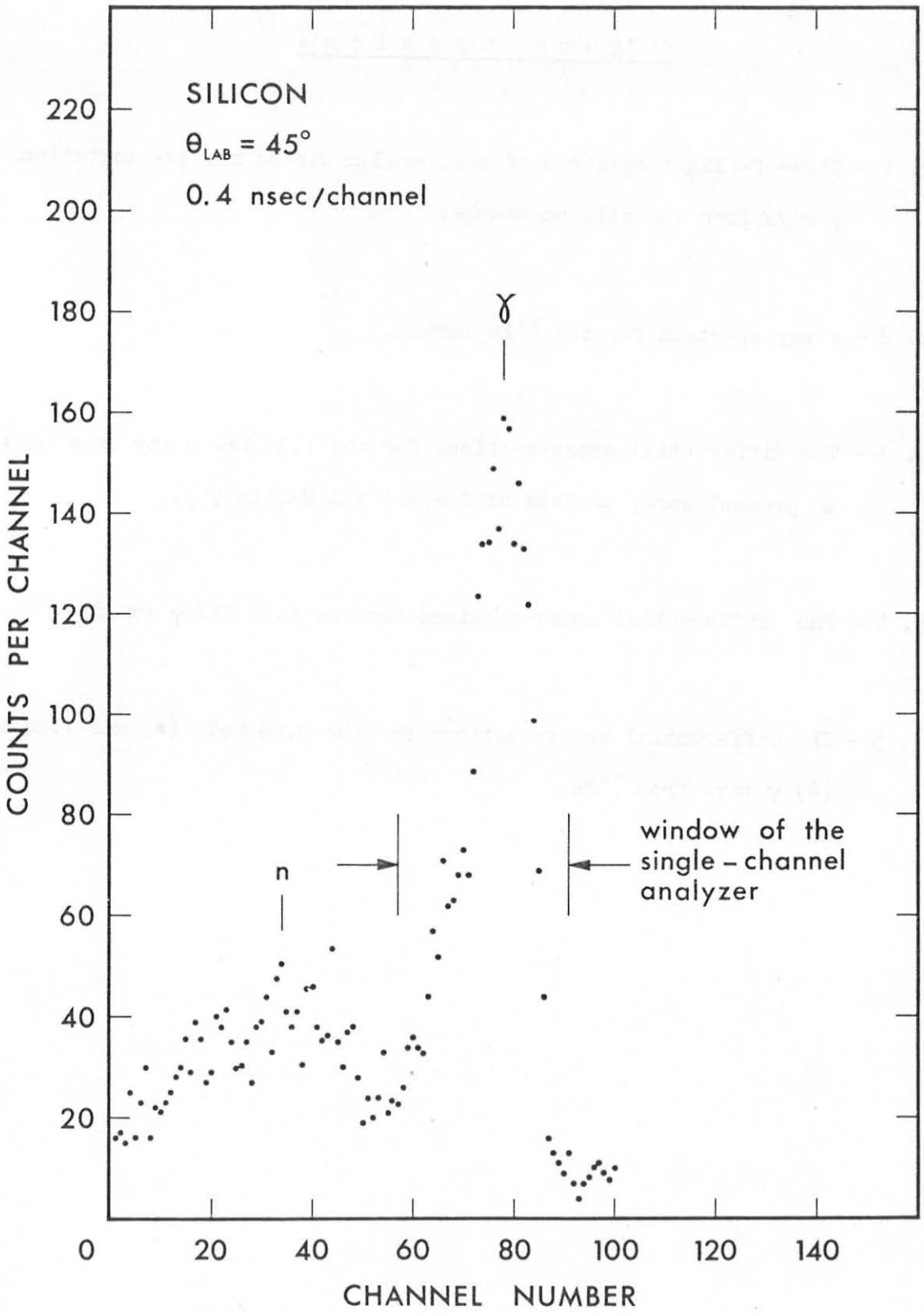
SILICON
$\theta_{LAB} = 45°$
0.4 nsec/channel
γ
n
window of the single – channel analyzer
COUNTS PER CHANNEL
CHANNEL NUMBER
0
20
40
60
80
100
120
140
160
180
200
220

Fig. 1

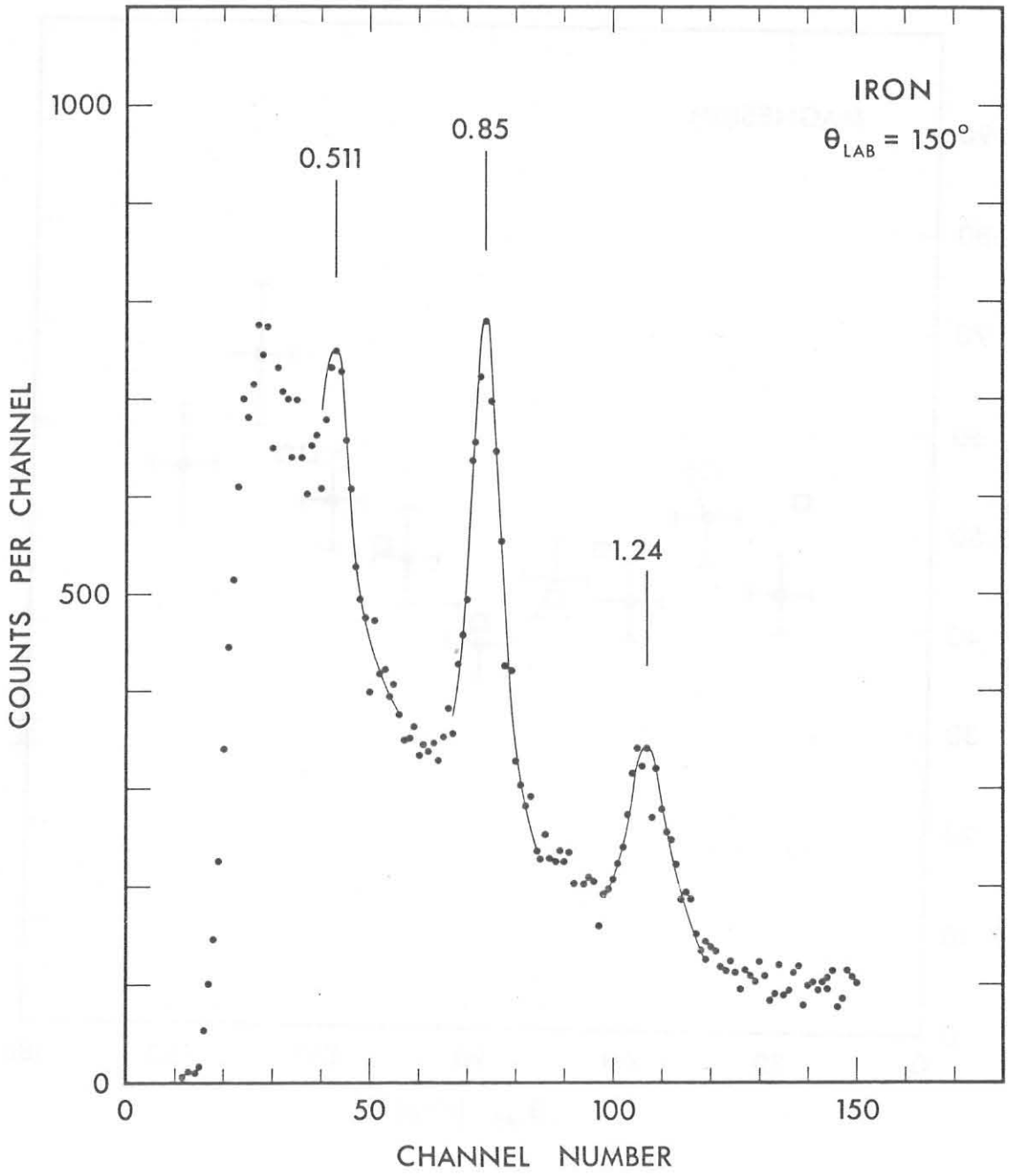
IRON
θ_{LAB} = 150°
0.511
0.85
1.24
1000
500
0
0
50
100
150
COUNTS PER CHANNEL
CHANNEL NUMBER

Fig. 2

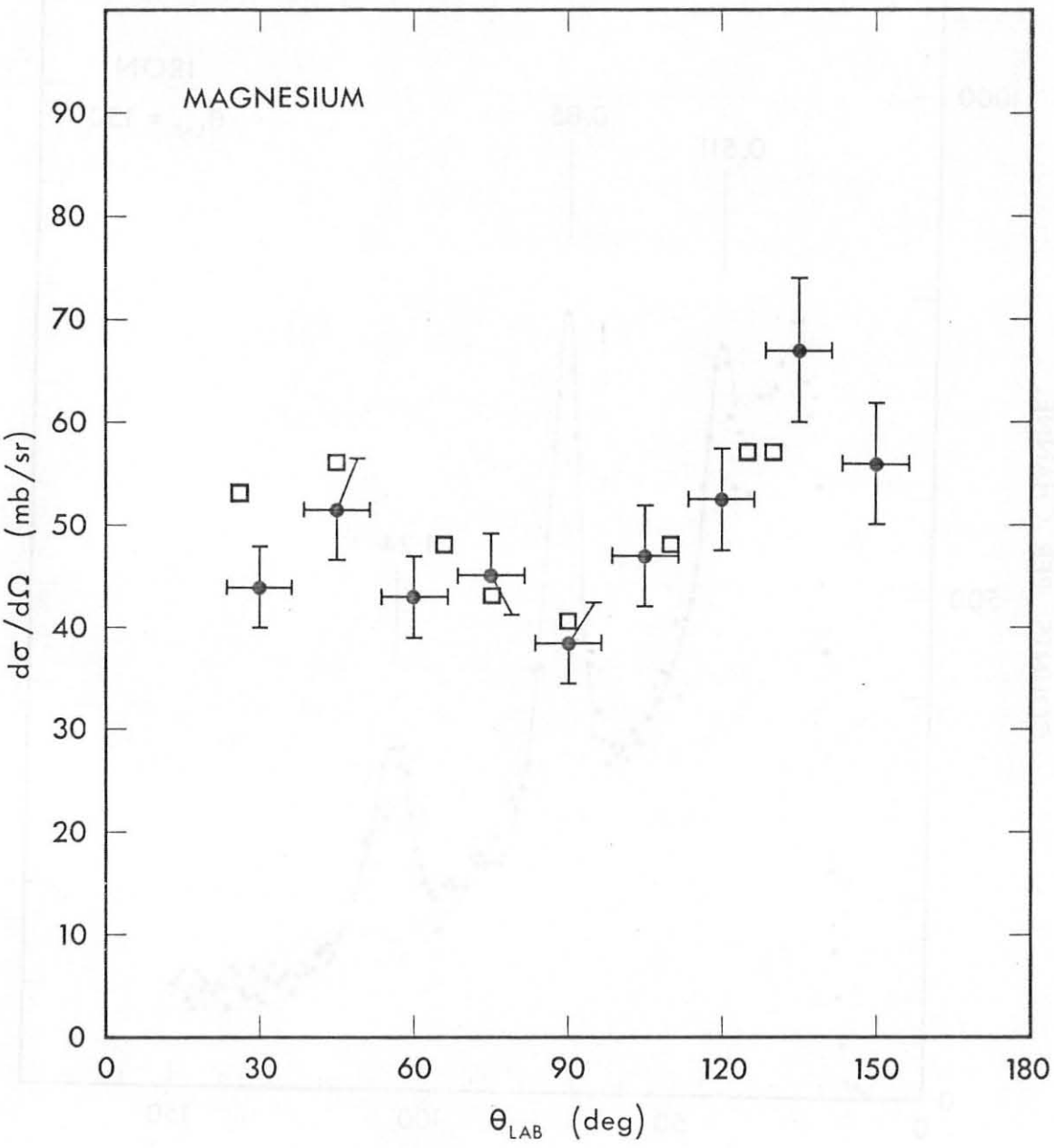
MAGNESIUM
dσ/dΩ (mb/sr)
θLAB (deg)
0
10
20
30
40
50
60
70
80
90
0
30
60
90
120
150
180

Fig. 3

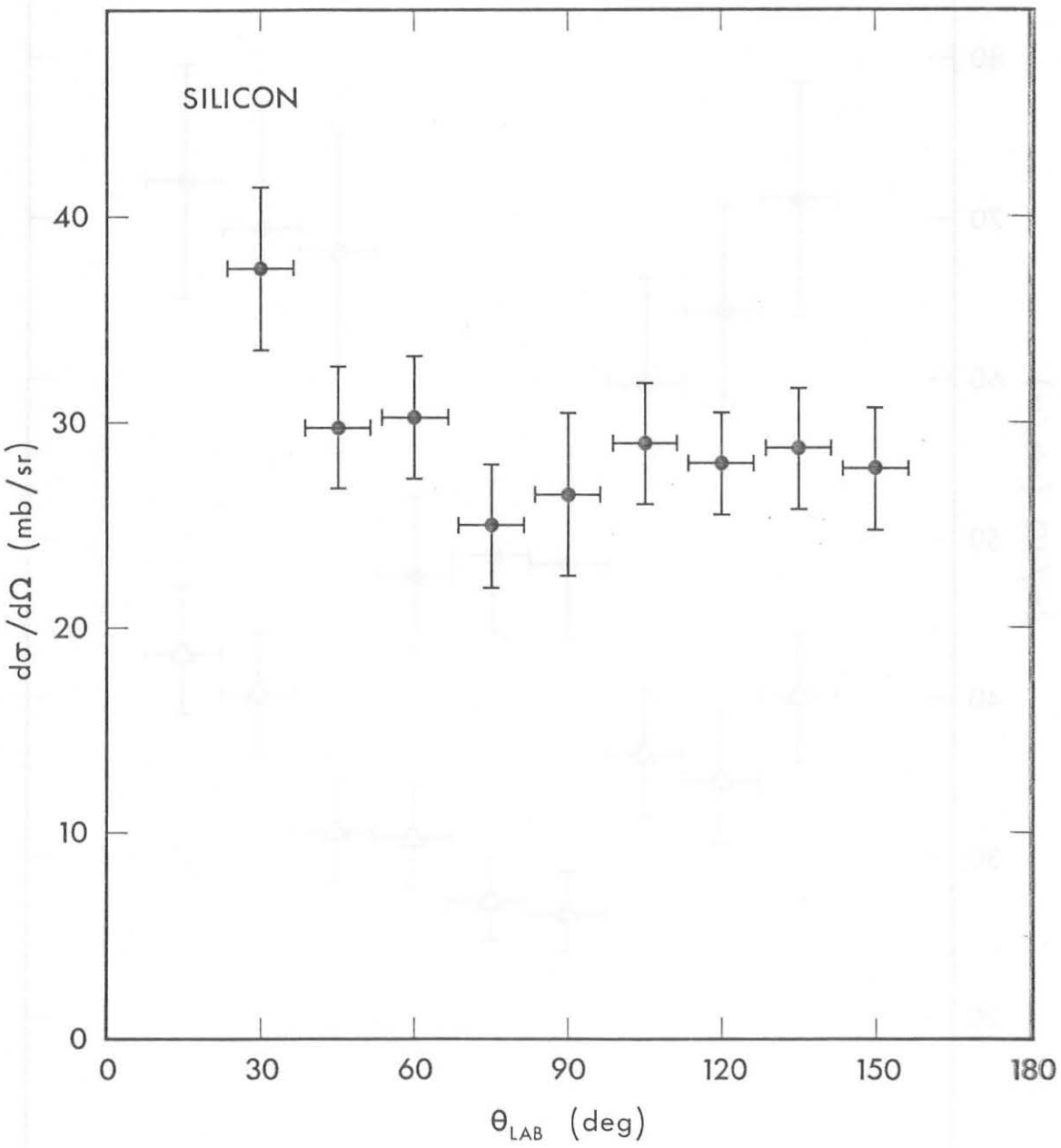

Fig. 4

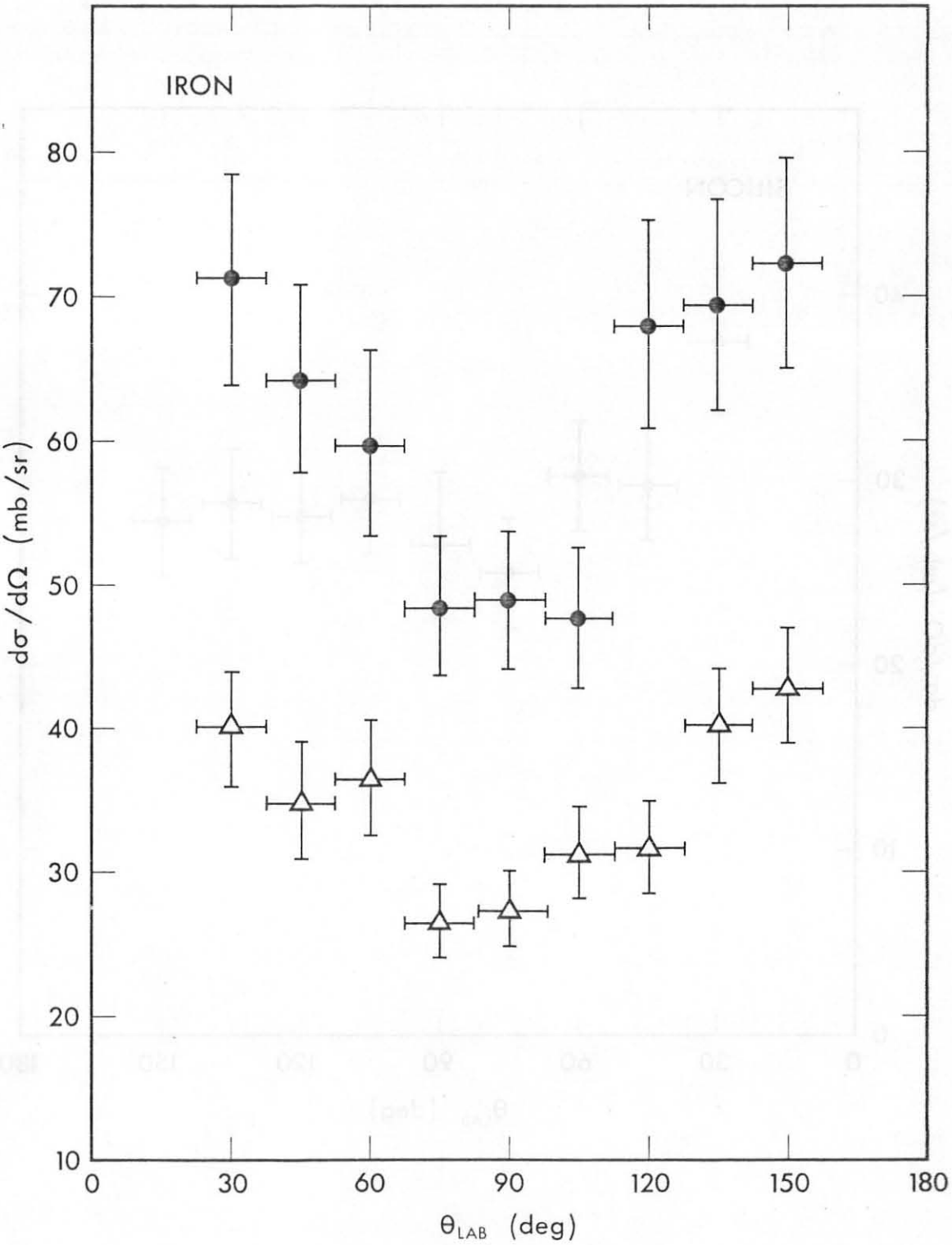
IRON
80
70
60
50
40
30
20
10
0
30
60
90
120
150
180
dσ/dΩ (mb/sr)
θLAB (deg)

Fig. 5